OPEN

Multilevel Analysis of the Neovascularization and Integration Process of a Nonvascularized Rectus Fascia Transplantation

Ewout Muylle, BSc,[1,2,3] Arne Maes, MSc,[4,5,6] Gert De Hertogh, MD, PhD,[1,7,8] Nele Van De Winkel, MD,[1,9,10] Greet Kerckhofs, PhD,[4,5,6,11] Antoine Dubois, MD,[1,2,12] Vincent Vandecaveye, MD, PhD,[13,14] Lieven Thorrez, PhD,[15] Ina Hennion, MSc,[15] Marie-Paule Emonds, MD, PhD,[16] Steven Pans, MD,[17] Nathalie P. Deferm, MD,[17] Diethard Monbaliu, MD, PhD,[1,2,12] Emilio Canovai, MD, PhD,[18] Tim Vanuytsel, MD, PhD,[1,19,20] Jacques Pirenne, MD, PhD,[1,2,12] and Laurens J. Ceulemans, MD, PhD[1,3,21]

Background. Failure to close the abdominal wall after intestinal transplantation (ITx) or multivisceral Tx remains a surgical challenge. An attractive method is the use of nonvascularized rectus fascia (NVRF) in which both layers of the donor abdominal rectus fascia are used as an inlay patch without vascular anastomosis. How this graft integrates over time remains unknown. The study aims to provide a multilevel analysis of the neovascularization and integration process of the NVRF. **Methods.** Three NVRF-Tx were performed after ITx. Clinical, radiological, histological, and immunological data were analyzed to get insights into the neovascularization and integration process of the NVRF. Moreover, cryogenic contrast-enhanced microfocus computed tomography (microCT) analysis was used for detailed reconstruction of the vasculature in and around the NVRF (3-dimensional histology). **Results.** Two men (31- and 51-y-old) and 1 woman (49-y-old) underwent 2 multivisceral Tx and 1 combined liver-ITx, respectively. A CT scan showed contrast enhancement around the fascia graft at 5 days post-Tx. At 6 weeks, newly formed blood vessels were visualized around the graft with Doppler ultrasound. Biopsies at 2 weeks post-Tx revealed inflammation around the NVRF and early fibrosis. At 6 months, classical 2-dimensional histological analysis of a biopsy confirmed integration of the fascia graft with strong fibrotic reaction without signs of rejection. A cryogenic contrast-enhanced microCT scan of the same biopsy revealed the presence of microvasculature, enveloping and penetrating the donor fascia. **Conclusions.** We showed clinical, histological, and microCT evidence of the neovascularization and integration process of the NVRF after Tx.

(*Transplantation Direct* 2024;10: e1624; doi: 10.1097/TXD.0000000000001624.)

Received 22 January 2024.

Accepted 5 February 2024.

[1] *Leuven Intestinal Failure and Transplantation (LIFT) Center, University Hospitals Leuven, Leuven, Belgium.*

[2] *Department of Abdominal Transplant Surgery, University Hospitals Leuven, Leuven, Belgium.*

[3] *Department of Chronic Diseases and Metabolism, Laboratory of Respiratory Diseases and Thoracic Surgery (BREATHE), KU Leuven, Leuven, Belgium.*

[4] *Department of Materials Engineering, KU Leuven, Leuven, Belgium.*

[5] *Biomechanics Lab, Institute of Mechanics, Materials and Civil Engineering, UCLouvain, Louvain-la-Neuve, Belgium.*

[6] *Pole of Morphology, Institute of Experimental and Clinical Research, UCLouvain, Brussels, Belgium.*

[7] *Department of Pathology, University Hospitals Leuven, Leuven, Belgium.*

[8] *Unit of Translational Cell- and Tissue Research, Department of Imaging and Pathology, KU Leuven, Leuven, Belgium.*

[9] *Department of Abdominal Surgery, University Hospitals Leuven, Leuven, Belgium.*

[10] *Department of Development and Regeneration, Unit of Urogenital, Abdominal and Plastic Surgery, KU Leuven, Leuven, Belgium.*

[11] *Prometheus Division of Skeletal Tissue Engineering, KU Leuven, Leuven, Belgium.*

[12] *Department of Microbiology, Immunology and Transplantation, KU Leuven, Leuven, Belgium.*

[13] *Department of Radiology, University Hospitals Leuven, Leuven, Belgium.*

[14] *Translational MRI Unit, Department of Imaging and Pathology, KU Leuven, Leuven, Belgium.*

[15] *Tissue Engineering Lab, Department of Development and Regeneration, KU Leuven, KULAK campus Kortrijk, Kortrijk, Belgium.*

[16] *Histocompatibility and Immunogenetics Laboratory, Belgian Red Cross-Flanders, Mechelen, Belgium.*

[17] *Department of Abdominal Surgery, Sint-Franciscusziekenhuis, Heusden-Zolder, Belgium.*

[18] *Nuffield Department of Surgical Sciences, University of Oxford, Oxford, United Kingdom.*

[19] *Department of Gastroenterology and Hepatology, University Hospitals Leuven, Leuven, Belgium.*

[20] *Department of Chronic Diseases and Metabolism, Translational Research Center for Gastrointestinal Disorders (TARGID), KU Leuven, Leuven, Belgium.*

[21] *Department of Thoracic Surgery, University Hospitals Leuven, Leuven, Belgium.*

Correspondence: Laurens J. Ceulemans, MD, PhD, Department of Thoracic Surgery and Lung Transplantation, University Hospitals Leuven/KU Leuven, Herestraat 49, 3000 Leuven, Belgium. (laurens.ceulemans@uzleuven.be); LinkedIn: www.linkedin.com/in/laurens-ceulemans-1190a7a1; Twitter: @CeulemansLJ.

Abstract presented at the 18th Biannual Congress of the Intestinal Rehabilitation and Transplant Association; June 30 to July 3, 2023; Chicago, IL, USA.

E.M. participated in research design and performed research and data analysis, constructed the figures and tables, and drafted the article. A.M. performed the research and data analysis (3D histology – cryogenic contrast-enhanced microCT analysis), constructed the figures and tables, participated in writing the article, and critically reviewed the article. G.D.H. performed of the research and data analysis (2-dimensional [2D] histology) and critically reviewed the article. N.V.D.W. and A.D. performed of the research and data analysis (surgical data)

Failure to close the abdominal wall is a major and frequently occurring surgical problem after intestinal transplantation (ITx), liver Tx (LTx), or multivisceral Tx (MvTx).[1] The majority of these patients have an extensive history of abdominal surgical procedures and suffer from ostomies, fistulas, and wound infections. Furthermore, edema of the graft caused by reperfusion and of the recipient contributes to the challenge of primarily closing the abdomen.[2] However, closure is key, because failure is associated with a 50% increase in morbidity (abdominal compartment syndrome, enterocutaneous fistulas, wound dehiscence, and graft loss) and a 10% increase in mortality.[2,3]

To overcome this challenge, several techniques have been developed, such as graft size reduction, tissue expanders, mesh application, or full-thickness vascularized abdominal wall Tx.[3-8] Although the latter holds the theoretical benefit of being used as a sentinel marker for intestinal rejection, there are conflicting reports, including intestinal rejection without skin rejection or the opposite.[2,9,10] Generally, these techniques are often complex with varying results or complications and performed after a time-consuming Tx procedure.

Therefore, a nonvascularized rectus fascia (NVRF) graft has been developed. By removing the muscle, both layers of the abdominal rectus fascia can be used as an inlay patch without vascular anastomosis.[11] It was first proposed by Gondolesi et al[12] in 2009 and, until now, has been described in >60 cases with an excellent short-term outcome (few complications, no fascia-related rejection, or death).[2] However, the neovascularization and integration process of the NVRF has not been reported to the best of our knowledge. The study aims to provide a detailed radiological and histological evaluation of NVRF in the short-term and mid-term in 3 patients. We also add novel insights into the clinical aspects, preservation, and immunogenicity of NVRF-Tx.

MATERIALS AND METHODS

Three patients underwent an NVRF-Tx in combination with an ITx or MvTx between September 2019 and September 2022 at University Hospitals Leuven, Belgium. Approval for patient reporting (MP023034) and tissue analysis (S67453) was granted by the local ethics committee.

Surgical Procedure

During procurement, a midline incision was made toward the anterior fascia, followed by lateral dissection until the oblique muscles. Starting from the cartilaginous arch of the chest, the rectus muscles were incised and the abdomen was opened lateral from these muscles. On both sides, the oblique muscles were transected up to the groins. Then, organ procurement was performed. Following cold flush, the bloc was removed and immediately prepared on the bench by opening the lateral side, cutting intersections, and removing muscular tissue. The donor was closed with a plastic sheet, covered by subcutaneous tissue and skin. Figure 1A and B shows the different layers of the rectus bloc with the anterior and posterior fascia sheet and peritoneum. After this, small lesions and perforating arteries were sutured with 3-0 Prolene and the graft was rinsed in cold saline. The NVRF graft was stored in 1 L Institut Georges Lopez-1 solution with topical antibiotics (gentamycin, 160 mg) within 3 bags and preserved on ice (0 °C).[13] The graft was stored in a fridge. At Tx, the NVRF was rinsed with polyvidone-iodine and NaCl 0.9%, tailored to the defect, and sutured, under moderate tension, in an inlay manner with several running 2-0 polypropylene monofilament threads (Prolene, Ethicon; Figure 1C–E). Then, if feasible, the NVRF was covered with subcutaneous tissue and skin. If not, vacuum-assisted closure (VAC) therapy was applied. Two subcutaneous drains were placed. The subcutaneous layer was closed with interrupted 2-0 Vicryl stitches and the skin with interrupted 2-0 Ethilon sutures.

Macroscopical, Radiological, and 2-Dimensional Histological Evaluation

Reoperations (including taking biopsies) and radiological imaging were only performed in case of a clinical indication. For this reason, time points of evaluation differ between patients. The macroscopical appearance of the NVRF was evaluated during each reoperation. Also, Doppler ultrasound (US) and computed tomography (CT) radiographical images were obtained at several time points post-Tx. If possible, biopsies were taken during reoperation at the interphase of the NVRF and native fascia for histological evaluation. Tissue samples were formalin-fixed, paraffin-embedded, cut into 5 µm thickness, and stained with hematoxylin and eosin (H&E) and Masson's trichrome. Immunohistochemistry for cluster of differentiation (CD)31 was performed using a monoclonal mouse anti-human CD31 antibody, clone JC70A (Agilent, Santa Clara, CA).

Three-dimensional X-Ray-based Histology Using (Cryogenic) Contrast-enhanced MicroCT

The sample preparation protocol for (cryo-)CECT is summarized in Supplemental Digital Content, Figure S1, and Table S1 (**SDC,** http://links.lww.com/TXD/A644).[14-17]

RESULTS

Recipient, donor, and surgical characteristics are summarized in Table S2 (**SDC,** http://links.lww.com/TXD/A644).

and critically reviewed the article. G.K. supervised the data analysis (3D histology – cryogenic contrast-enhanced microCT analysis) and critically reviewed the article. V.V. and S.P. performed the research and data analysis (radiological data) and critically reviewed the article. L.T. and I.T. performed data analysis and interpretation (2D histology) and critically reviewed the article. M.-P.E. performed the research and data analysis (immunological data) and critically reviewed the article. N.P.D., D.M., and E.C. performed the research and data analysis (surgical data) and critically reviewed the article. T.V. performed the research and data analysis (clinical data) and critically reviewed the article. J.P. supervised the study and critically reviewed the article. L.J.C. designed and supervised the study and drafted the article.

The authors declare no conflicts of interest.

L.J.C. and L.T. were granted a Translational Biomedical Research Fund grant from KU Leuven. L.J.C. is appointed as senior clinical investigator for Fonds Wetenschappelijk Onderzoek Vlaanderen.

The (cryo-)microCT work presented in this article was funded by an Actions de Recherche Concertées grant of UCLouvain.

Supplemental digital content (SDC) is available for this article. Direct URL citations appear in the printed text, and links to the digital files are provided in the HTML text of this article on the journal's Web site (www.transplantationdirect.com).

ISSN: 2373-8731

DOI: 10.1097/TXD.0000000000001624

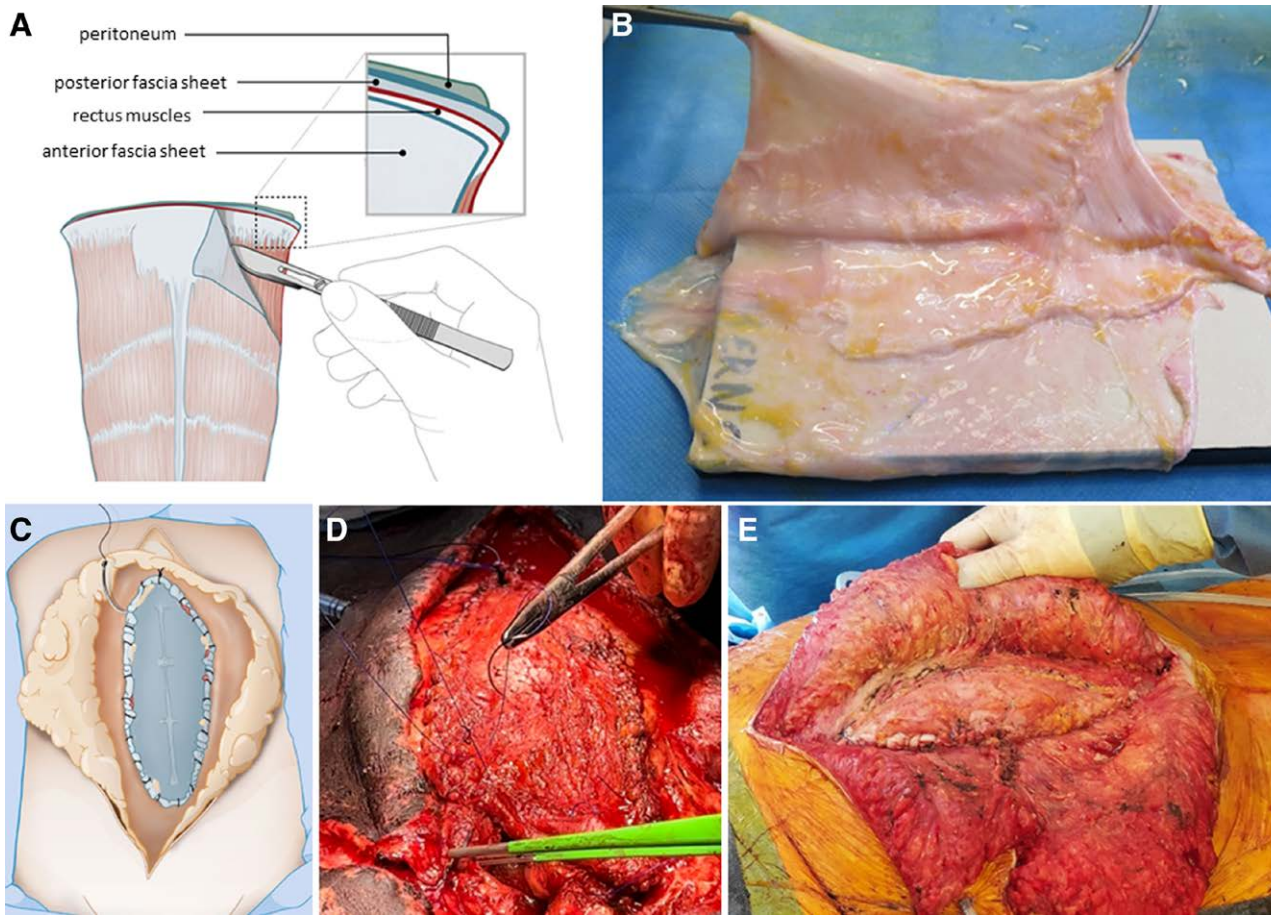

FIGURE 1. Surgical procedure of NVRF procurement and transplantation. A, Illustration of the 4 layers of the rectus bloc consisting of (from anterior to posterior) anterior fascia, rectus muscles, posterior fascia, and peritoneum (Data from Muylle E, Van De Winkel N, Hennion I, et al., Abdominal Wall Closure in Intestinal and Multivisceral Transplantation. Gastroenterol Clin N Am. 2024. Available online. https://doi.org/10.1016/j.gtc.2023.12.001; with permission. B, Appearance of prepared rectus fascia with anterior and posterior sheet pretransplantation. C, Illustration of the position of the NVRF in the recipient posttransplantation. D, Intraoperative image of NVRF that is sutured to the native rectus fascia of the recipient with a running suture. E, Appearance of the NVRF posttransplantation into the recipient. NVRF, nonvascularized rectus fascia.

Patient 1

Clinical Description

A 49-y-old woman (height: 168 cm; weight: 77.5 kg; blood group [BG]: A^-; cytomegalovirus [CMV]: positive) had a history of essential thrombocytosis and was a carrier of janus kinase 2 gene mutation. The patient was diagnosed with acute superior mesenteric artery thrombosis resulting in subtotal enterectomy followed by tube duodenum-sigmoidostomy leading to ultra-short bowel syndrome. Three years later, she underwent combined pancreas-intestinal-kidney Tx. However, she developed severe, grade 3 acute cellular rejection. Prolonged antirejection treatment was unsuccessful, resulting in complete intestinal desquamation and ongoing candida sepsis. The bowel and pancreas grafts were explanted. The patient was relisted 2.5 months later for combined liver-intestinal-pancreas Tx, 1 year after the first Tx. The donor of this graft was a 16-y-old girl (height: 168 cm; weight: 52 kg; BG: A^+; CMV: positive) who suffered posttraumatic brain edema. Post-Tx, primary closure of the abdominal wall could not be attained, resulting in a 9 × 24 cm defect. To cover this, an NVRF of the same donor was used. Primary skin closure could be performed and an end-ileostomy was constructed. She had an uneventful recovery without infection, abdominal bulging, or herniation. Six months post-Tx, intestinal continuity was restored and biopsies of the NVRF were taken. Macroscopically, the NVRF had shrunken and was well integrated. To date, 50 months post-Tx, no bulging or herniation was observed.

Radiological Findings

At 5 days post-Tx, CT scan revealed contrast enhancement around the right side of the graft (Figure 2A), which intensified at 1 month and was present on both sides of the graft (Figure 2B). Six weeks post-Tx, Doppler US showed the presence of newly formed blood vessels around the NVRF graft with blood flow from the native fascia to the graft (Figure 2C).

Classical 2-Dimensional Histological Findings

Biopsies at 6 months post-Tx show the NVRF graft appearing as an eosinophilic mass representing precipitated collagen fibers (Figure 2D–F). The graft is surrounded by fibrotic, connective tissue in which small, newly formed blood vessels are visible, surrounded by inflammatory cells (mainly plasma cells and a smaller number of lymphocytes). Some of these blood vessels penetrate the NVRF, which is confirmed by CD31 staining showing the presence of endothelial cells within the graft (Figure 2G). In different locations, foreign-body giant cells are present without signs of rejection (Figure 2H). At the interphase of the donor

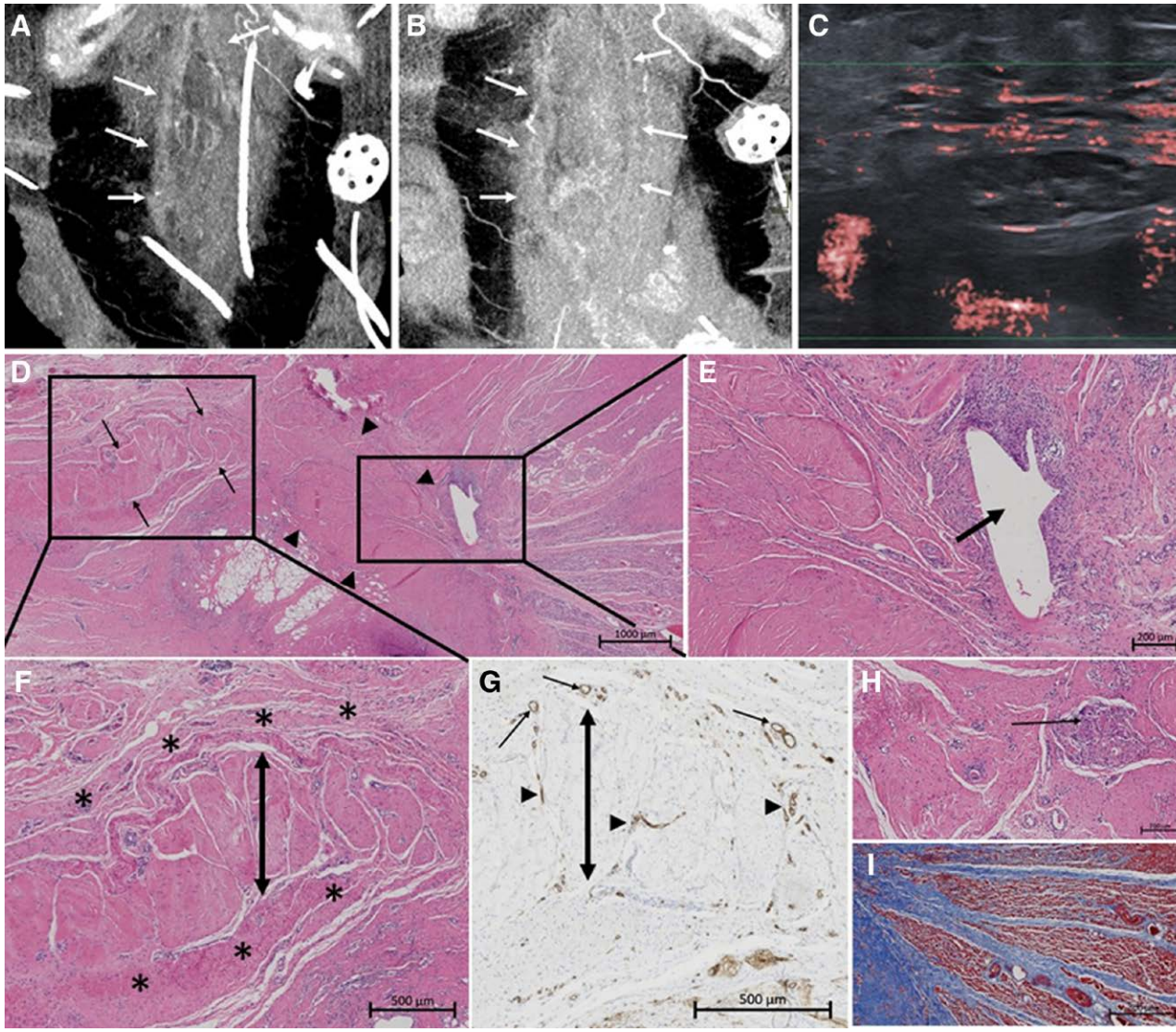

FIGURE 2. Radiological and classical 2-dimenional histology findings of NVRF in case 1. A. CT scan showing the NVRF 5 days posttransplantation. An increase in contrast is seen around the fascia graft, mainly on the right side (white arrows). B, CT scan showing the NVRF, 1 month posttransplantation. The CT image is shown reconstructed in the coronal plane over the anterior abdominal wall in maximum intensity projection of the arterial phase scan. The contrast enhancement around the NVRF is raised compared with the previous CT scan and is present on both sides of the fascia graft. C, Abdominal Doppler US at 6 weeks posttransplantation showing the presence of newly formed blood vessels around the NVRF graft. D, General overview of the NVRF graft at the interphase with the native fascia. The edges of the donor NVRF are indicated with arrows. The arrowheads show another part of the donor NVRF that is sutured against the recipient's fascia and muscle tissue (H&E staining). E, Detail of a surgical stitch (arrow) close to the interphase of donor and recipient fascia. Around the stitch, highly cellular fibrotic tissue with blood vessels is present (H&E staining). F, Detail of the NVRF graft and fibrotic reaction. The NVRF (indicated by the double arrow) appears as an eosinophilic mass consisting of precipitated collagen bundles of fascia tissue. The graft is surrounded by the fibrotic reaction, indicated with asterisks, consisting of newly formed connective tissue with inflammatory cells (H&E staining). G, Immunohistochemistry analysis for CD31 of the NVRF. The arrows indicate several vessels at the interphase of the fibrotic reaction of the recipient and the NVRF. The arrow heads are showing blood vessels running through the NVRF. H, Detail of a foreign-body reaction in the direct neighborhood of the NVRF. The arrow indicates a foreign-body giant cell (H&E staining). I, Detail of muscle tissue bundles, colored in red, of the recipient's abdominal wall becoming atrophic at the interphase with the NVRF (Masson's trichrome staining). CD, cluster of differentiation; CT, computed tomography; H&E, hematoxylin and eosin; NVRF, nonvascularized rectus fascia.

fascia and native abdominal wall, the skeletal muscle appears atrophic (Figure 2I). Around a hole in the tissue, representing the suture location, cellular connective tissue with unorganized collagen fibers and lymphocytes is observed (Figure 2E).

Three-dimensional Histology Findings Using (Cryo-)CECT Analysis

On the overview CECT images of the same biopsy, the NVRF could be recognized by 2 bright sheets encapsulating the graft (Figure 3A). Farther away from the acceptor side, however, these sheets could not be observed. CECT analysis also revealed the presence of blood vessels enveloping and entering the donor NVRF (Figure 3B). Using cryo-CECT resulted in a more detailed delineation of the blood vessel wall and also allowed to visualize the collagen fiber bundles inside the donor fascia (Figure 3C). By aligning the (cryo-)CECT slices to the corresponding 2-dimensional (2D) histological sections (**Figure S1, SDC,** http://links.lww.com/TXD/A644), visualization of the blood vessels and collagen fiber bundles

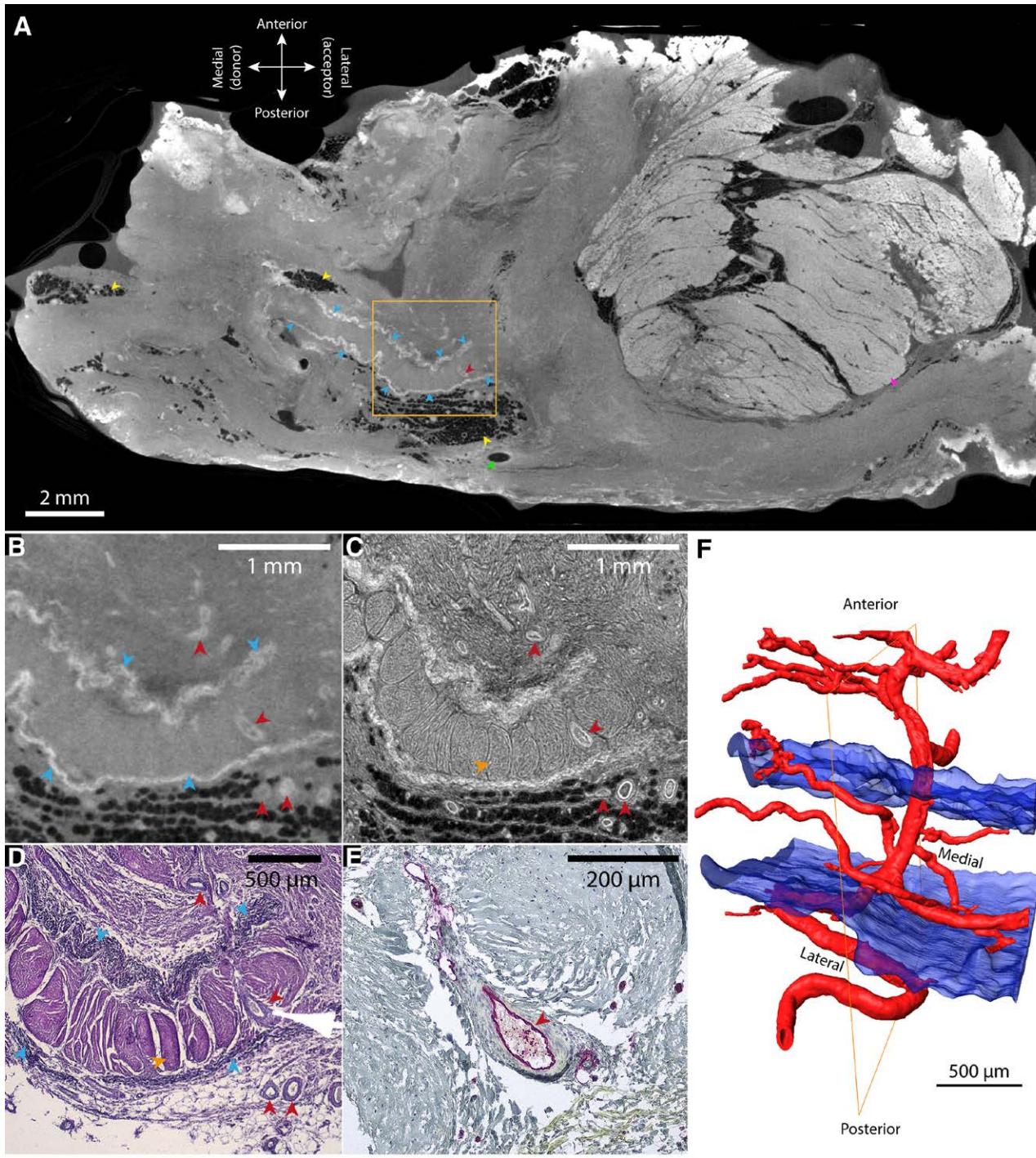

FIGURE 3. Three-dimensional histology findings using CECT and cryo-CECT analysis of NVRF in case 1. A, Transverse CECT slice through the biopsy, containing the NVRF (blue arrows), penetrating blood vessel (red arrow), suturing wire (green arrow), adipose tissue (yellow arrows), and muscle tissue (pink arrow). B, A magnification (orange rectangle in A) showing the NVRF (blue arrows) and the penetrating blood vessel (red arrows) C, Cryo-CECT slice corresponding to (B), showing in more detail the blood vessels (red arrows) and the collagen fiber bundles within the NVRF (orange arrow). D and E, Histological sections (H&E staining in D, and CD31 immunohistochemistry in E) corresponding to (B and C), validating the (cryo-)CECT visualization of the blood vessels (red arrows), the NVRF (blue arrows), and the collagen fiber bundles (orange arrow). F, Three-dimensional volume rendering, based on the cryo-CECT data, of the same penetrating blood vessel (red arrows) showing that it originates from the outside of the NVRF and runs through the whole width of the NVRF graft (indicated by the encapsulating sheets in blue). CD, cluster of differentiation; cryo-CECT, cryogenic contrast-enhanced microfocus computed tomography; H&E, hematoxylin and eosin; NVRF, nonvascularized rectus fascia.

could be confirmed (Figure 3D and E). Segmentation and 3D rendering of the blood vessels showed that they penetrated the NVRF from the native fascia, as well as from the peritoneal and subcutaneous side (Figure 3F). A video of the 3D reconstruction is included in Supplemental Digital Content (**SDC,** http://links.lww.com/TXD/A644).

Patient 2

Clinical Description

A 51-y-old man (height: 163 cm; weight: 52.4 kg; BG: A+; CMV: negative) with an intestinal infarction resulting in extended resections, short bowel syndrome, and intestinal failure-associated liver disease received an MvTx (stomach, pancreas, liver, and small bowel) from a 26-y-old female donor (height: 167 cm; weight: 51 kg; BG: A+; CMV: negative). After Tx, an NVRF of the same donor was used to cover a fascial defect (8.5 × 22 cm). Due to intra-abdominal fluid collection, an explorative laparotomy was required 52 hours later. A midline incision over the linea alba of the NVRF was performed. Macroscopically, no loosening of the NVRF graft was observed and biopsies were taken. Two weeks later, a second explorative laparotomy was performed for fever and suspicion of the formation of a mycotic aneurysm. Macroscopically, there were no signs of an overt intra-abdominal infection and neovascularization could be observed on the peritoneal side. On the cranial side of the wound, the skin could not be closed because of recipient's edema and skin necrosis and needed to be resected. Therefore, primary skin closure was not possible, so a VAC pump with intermittent suction (–75 mm Hg) was applied. Two weeks later, secondary skin closure was attained. Two months later, imaging revealed multiple hepatic lesions and a disseminated mesothelioma was diagnosed. Two weeks later, the patient died.

2D Histological Findings

Biopsies taken at 2 weeks post-Tx reveal a large number of neutrophilic granulocytes in the direct neighborhood of blood vessels, suggesting inflammation in the connective tissue around the fascia. The blood vessels are congested because of inflammation. Deposition of recently formed connective tissue around the graft can be observed (**Figure S2, SDC,** http://links.lww.com/TXD/A644).

Patient 3

Clinical Case Description

A 31-y-old man (height: 175 cm; weight: 55 kg; BG: O+; CMV: positive) with a history of congenital biliary atresia and previous Kasai was referred for MvTx. The donor was a 53-y-old woman (height: 170 cm; weight: 70 kg; BG: O+; CMV: negative). The fascia could be primarily closed. Nine days later, reoperation was performed for an intra-abdominal hematoma and volvulus. Eleven days later, reoperation was performed for the kinking of the superior mesentery artery. An iliac-ileocolic bypass was constructed and an abdominal wall defect (7 × 24 cm) remained, requiring an NVRF-Tx. Since this reoperation was anticipated, a third-party fascia was procured 4 days earlier and preserved for 104 hours. The NVRF donor was a 33-y-old man (height: 180 cm; weight: 75 kg; BG: A+; CMV: negative). As the fascia could not be covered by skin, VAC therapy (–75 mm Hg) was applied. Six days post-Tx, anti-A titer was rising compared with the natural and immune antibody titers on the day of Tx suggesting formation of de novo–specific antibodies against this third-party fascia graft (ABO-mismatch). Twelve days after the NVRF-Tx, the patient died of a rupturing mycotic aneurysm of the aortic tube. At reintervention, the fascia looked macroscopically intact without signs of rejection.

DISCUSSION

This clinical series of 3 NVRF-Tx provides, for the first time to our knowledge, an analysis of the neovascularization and integration process of the graft into the recipient's abdominal wall. We used (cryo-)CECT analysis for detailed and high-resolution 3D reconstruction of blood vessels within and outside the NVRF. Moreover, this analysis was used to guide sample sectioning for 2D histology analysis. (Cryo-)CECT has not been used in this clinical context before. Furthermore, we describe new clinical and immunological findings about using NVRF-Tx in the ITx setting.

On CT scan, contrast enhancement of the tissue around the graft was observed from 5 days post-Tx and further increased over time, showing the progressive neovascularization process around the NVRF. On biopsies, classical 2D histological assessment using H&E staining revealed the formation of a dense fibrotic reaction originating from the tissue around the fascia graft. Deposition of fibrotic tissue around the graft is already present in the second week post-Tx. A limited number of foreign-body giant cells and lymphocytes are found in this fibrotic tissue. Clear signs of neovascularization within the NVRF could be visualized on CD31 stained 2D sections 6 months post-Tx. This neovascularization and fibrotic process originates from all sides as shown in the (cryo-)CECT data sets: native fascia, subcutaneous layer, and peritoneum. Interestingly, newly formed, highly vascularized connective tissue was observed around the surgical stitches, suggesting that this foreign material could stimulate the neovascularization and integration process. The newly formed blood vessels branch also within the NVRF graft.

In contrast to NVRF-allograft, the use of a free fascia lata allograft (FLA) has already been described as an alternative for prosthetic materials in hernia repair.[17] Tiengo et al[17] provided in a retrospective series of 21 patients some radiological evidence of the good integration of FLA for abdominal wall repair. However, no histological data were reported in this study.

Sekine et al[18] described the use of an autologous fascia graft that showed signs of neovascularization based on MRI findings, 3 months after surgery, without histopathological proof. In experimental studies in rabbits, Disa et al[19] reported that in autologous fascia patches originating from the thoracodorsal fascia used for abdominal reconstruction, a fine vasculature was shown to interdigitate with the graft post-Tx. Also, intact fascial elements and architecture preservation were found on histological sections after 3 and 6 weeks of healing. Healing after allograft tendon Tx follows a certain histological process consisting of exudation, graft necrosis, neovascularization, fibroblastic invasion, collagen synthesis, and alignment of the mature fibers along the direction of stress.[20] Similar phases are present during the integration process of an NVRF graft post-Tx. With the combined histological findings of the first 2 patients, we could show the neovascularization, fibroblastic invasion, and collagen synthesis phase.

The last time point at which we were able to assess the graft histologically was 6 months post-Tx, when the fascia graft was still recognizable. However, in the context of FLA, the graft is expected to be indistinguishable 1 year post-Tx.[17,21] In one study in which FLAs were used in rabbit cornea, donor fibroblasts seemed to disappear 1 week post-Tx.

Fibroblasts of the host repopulated fascia allograft within 3 weeks.[22,23] This supports the idea that the transplanted allograft is a temporary template, against which fibrotic tissue is developed. This process renders strength to the graft, because collagen fibers mature in the direction of the forces the allograft is subjected to. The graft undergoes neovascularization, invasion of fibroblasts, and finally, fibroplasia, and it is expected to be resorbed completely and replaced by the fibrotic tissue of the recipient over months.[17,20] Zurek et al[21] illustrated the same mechanism in which an extensive histological assessment was performed following the use of FLA in the context of multiple gingival recessions. It also has been suggested in the literature that FLAs have good resistance to bacterial infections and thus could be used in contaminated wounds.[24]

Since fascia tissue is mainly composed of extracellular matrix, it is generally assumed that the use of fascia allograft could not result in additional challenges in terms of tolerance and integration in comparison with fascia autograft.[11,12] Therefore, it is considered as low immunogenic and, consequently, ABO-matching would not be needed.[22] Indeed, in our patients, no signs of rejection against the NVRF were observed. However, patients were on immunosuppressants because of the solid organ Tx that preceded the NVRF-Tx. Interestingly, it is shown that FLA tissue remains antigenic even after freeze-drying and solvent treatment.[22] Moreover, in our third patient who received a non-ABO-matched third-party fascia, blood serum taken at 6 days after NVRF-Tx, revealed a slightly elevated anti-A titer, which could be interpreted as donor-specific antibodies. It is difficult to determine whether this elevation of anti-ABO antibodies is clinically important because long-term follow-up was not possible. In 1 case of the Cambridge experience, third-party fascia-specific antibodies were increased in blood, taken at 48 days post-Tx.[2,25] Based on these findings, the immunogenicity of the NVRF graft and the clinical implication of fascia-specific antibodies should be investigated further, ideally in animal models. A mild inflammatory reaction because of the antigenicity of the graft might be beneficial for the integration process of NVRF. This could potentially stimulate the fibrotic reaction and neovascularization, contributing to the graft strength.[22,26]

Another biocompatible option for abdominal wall reconstruction after ITx is the use of biological meshes such as acellular dermal allografts (ADAs). These are easy to work with, being suitable for every kind of defect. In contrast to the NVRF, primary skin closure is required, avoiding the use of VAC therapy to prevent mesh' degradation. Another consideration of ADAs is the cost ($5000–$10 000).[6]

Furthermore, we report interesting clinical observations about NVRF-Tx. The 3 grafts were preserved at 0 °C. There is no consensus about how long fascia can safely be preserved.[27,28] Several cold ischemia times have been reported up to 21 days.[4,12] Possibly, the graft could even be cryopreserved.[4] We also report the successful use of a third-party fascia (preservation time: 104 hours), resulting in a good macroscopical integration after 1 month. Further follow-up was not possible because of the death of the patient, unrelated to the NVRF-Tx. Other clinical observations were the successful application of the VAC therapy on top of the fascia graft and reoperation through midline incision of the donor NVRF, as previously reported.[11] Important to note is the ability of VAC therapy to promote neovascularization and promote sprouting of the new blood vessels.[29] In the future, we will increase the suction up to −125 mm Hg. In our 3 cases, orifices of perforating arteries were closed with polypropylene sutures, as described by Farinelli et al,[4,12] suturing the anterior and posterior sheets of fascia together. This may prevent the formation of a seroma between the 2 fascia layers.

In conclusion, this case series provides radiological, 2D and 3D histological evidence of the integration and neovascularization process of NVRF in the setting of ITx, corresponding to a fibrotic reaction.

ACKNOWLEDGMENTS

The authors thank the Leuven Intestinal Failure and Transplant team for treating our patients and pushing the field forward.

REFERENCES

1. Cloonan MR, Fortina CA, Mercer DF, et al. Failure of abdominal wall closure after intestinal transplantation: identifying high-risk recipients. *Clin Transplant*. 2019;33:e13713.
2. Janssen Y, Van De Winkel N, Pirenne J, et al. Allotransplantation of donor rectus fascia for abdominal wall closure in transplant patients: a systematic review. *Transplant Rev (Orlando)*. 2021;35:100634.
3. Ceulemans LJ, Deferm NP, Miserez M, et al. The role of osmotic self-inflatable tissue expanders in intestinal transplant candidates. *Transplant Rev (Orlando)*. 2016;30:212–217.
4. Farinelli PA, Rubio JS, Padín JM, et al. Use of nonvascularized abdominal rectus fascia after liver, small bowel, and multiorgan transplantation: long-term follow-up of a single-center series. *Transplant Proc*. 2017;49:1810–1814.
5. Gerlach UA, Pascher A. Technical advances for abdominal wall closure after intestinal and multivisceral transplantation. *Curr Opin Organ Transplant*. 2012;17:258–267.
6. Mangus RS, Kubal CA, Tector AJ, et al. Closure of the abdominal wall with acellular dermal allograft in intestinal transplantation. *Am J Transplant*. 2012;12(Suppl 4):S55–S59.
7. Watson MJ, Kundu N, Coppa C, et al. Role of tissue expanders in patients with loss of abdominal domain awaiting intestinal transplantation. *Transpl Int*. 2013;26:1184–1190.
8. Levi DM, Tzakis AG, Kato T, et al. Transplantation of the abdominal wall. *Lancet*. 2003;361:2173–2176.
9. Gerlach UA, Vrakas G, Sawitzki B, et al. Abdominal wall transplantation: skin as a sentinel marker for rejection. *Am J Transplant*. 2016;16:1892–1900.
10. Selvaggi G, Levi DM, Cipriani R, et al. Abdominal wall transplantation: surgical and immunologic aspects. *Transplant Proc*. 2009;41:521–522.
11. Cassar N, Cortes-Cerisuelo M, Bambridge C, et al. The difficult abdominal closure after paediatric intestinal transplantation: use of abdominal rectus muscle fascia and literature review. *Pediatr Transplant*. 2019;23:e13473.
12. Gondolesi G, Selvaggi G, Tzakis A, et al. Use of the abdominal rectus fascia as a nonvascularized allograft for abdominal wall closure after liver, intestinal, and multivisceral transplantation. *Transplantation*. 2009;87:1884–1888.
13. Canovai E, Oltean M, Herlenius G, et al. IGL-1 as a preservation solution in intestinal transplantation: a multicenter experience. *Transpl Int*. 2020;33:963–965.
14. Kerckhofs G, Stegen S, van Gastel N, et al. Simultaneous three-dimensional visualization of mineralized and soft skeletal tissues by a novel microCT contrast agent with polyoxometalate structure. *Biomaterials*. 2018;159:1–12.
15. Leyssens L, Pestiaux C, Kerckhofs G. A review of ex vivo X-ray microfocus computed tomography-based characterization of the cardiovascular system. *Int J Mol Sci*. 2021;22:3263.
16. de Bournonville S, Vangrunderbeeck S, Ly HGT, et al. Exploring polyoxometalates as non-destructive staining agents for contrast-enhanced

microfocus computed tomography of biological tissues. *Acta Biomater*. 2020;105:253–262.
17. Tiengo C, Giatsidis G, Azzena B. Fascia lata allografts as biological mesh in abdominal wall repair. *Plast Reconstr Surg*. 2013;132:631e–639e.
18. Sekine Y, Sugo H, Iwanaga N, et al. Relaparotomy two years after incisional hernia repair using a free fascia lata graft. *Case Rep Surg*. 2020;2020:1769404.
19. Disa JJ, Klein MH, Goldberg NH. Advantages of autologous fascia versus synthetic patch abdominal reconstruction in experimental animal defects. *Plast Reconstr Surg*. 1996;97:801–806.
20. Gibbons MJ, Bartolozzi AR. Anterior cruciate ligament reconstruction using allografts: a review of the important issues. *Oper Tech Orthop*. 1992;2:76–85.
21. Zurek J, Dominiak M, Tomaszek K, et al. Multiple gingival recession coverage with an allogeneic biostatic fascia lata graft using the tunnel technique-histological assessment. *Ann Anat*. 2016;204:63–70.
22. FitzGerald MP, Mollenhauer J, Brubaker L. The antigenicity of fascia lata allografts. *BJU Int*. 2000;86:826–828.
23. Crawford JS. Nature of fascia lata and its fate after implantation. *Am J Ophthalmol*. 1969;67:900–907.
24. Park TH. The versatility of tensor fascia lata allografts for soft tissue reconstruction. *Int Wound J*. 2023;20:784–791.
25. Amin I, Canovai E. Closing the abdomen: update on the current surgical toolkit. *Curr Opin Organ Transplant*. 2022;27:131–136.
26. Peacock EE. Subcutaneous extraperitoneal repair of ventral hernias: a biological basis for fascial transplantation. *Ann Surg*. 1975;181:722–727.
27. Fortunato AC, Pinheiro RS, Matsumoto CS, et al. Techniques for closing the abdominal wall in intestinal and multivisceral transplantation: a systematic review. *Ann Transplant*. 2022;27:1–14.
28. Justo I, Marcacuzco A, Caso O, et al. Use of nonvascularized fascia in liver transplantation. *Transplant Proc*. 2020;52:1468–1471.
29. Ma Z, Shou K, Li Z, et al. Negative pressure wound therapy promotes vessel destabilization and maturation at various stages of wound healing and thus influences wound prognosis. *Exp Ther Med*. 2016;11:1307–1317.